Structural Engineering and Mechanics, Vol. 20, No. 2 (2005) 225-239
DOI: http://dx.doi.org/10.12989/sem.2005.20.2.225

Mode III fracture analysis of piezoelectric materials by Trefftz BEM

Qing-Hua Qin†

Department of Engineering, Australian National University, Acton ACT 0200, Australia

(Received November 10, 2004, Accepted March 14, 2005)

Abstract. Applications of the Trefftz boundary element method (BEM) to anti-plane electroelastic problems are presented in this paper. Both direct and indirect methods with domain decomposition are discussed in details. Each crack is treated as semi-infinite thin slit defined in a subregion, for which a particular solution of the anti-plane problem, satisfying exactly the crack-face condition, is derived. The stress intensity factors defined at each crack tip can be directly computed from the coefficients of the particular solution. The performance of the proposed formulation is assessed by two examples and comparison is made with results obtained by other approaches. The Trefftz boundary element approach is demonstrated to be suitable for the analysis of the anti-plane problem of piezoelectric materials.

Key words: Trefftz method; piezoelectric; anti-plane; boundary element.

1. Introduction

During the past decades Trefftz approach, introduced by Trefftz (1926), has been considerably improved and has now become a highly efficient computational tool for the solution of complex boundary value problems. For the Trefftz boundary element method, Cheung *et al.* (1989) developed a direct formulation for solving two-dimensional potential problem. Kita *et al.* (1999) studied the same problem by the direct formulation and domain decomposition approach. Portela and Charafi (1997) applied Trefftz Boundary element formulation to potential problems with thin internal or edge cavities. Sladek *et al.* (2002) presented a global and local Trefftz boundary integral approach to solve Helmholtz equation. Domingues *et al.* (1999) extended the Trefftz boundary element approach to the analysis of linear elastic fracture mechanics. Recently, Qin (2003) applied trefftz finite element method to anti-plane problems of piezoelectric materials. Most of the developments in the field can also be found in (Kita 1995, Qin 2000).

In the present paper, we confine our attention to the applications of Trefftz boundary element method to anti-plane electroelastic problems which is different from the Trefftz finite element method presented in our previous work (Qin 2003). Both direct and indirect methods are discussed in details. Special functions that satisfy traction-free conditions along crack faces are used as trial functions for those subdomains containing a crack. Numerical results to mode III problem obtained by the Trefftz BEM are compared with those obtained from other approaches.

† Professor, E-mail: qinghua.qin@anu.edu.au

2. Basic formulations for anti-plane problem

2.1 Basic equations

In the case of anti-plane shear deformation involving only out-of-plane displacement u_z and in-plane electric fields, we have

$$u_x = u_y = 0, \quad u_z = u_z(x, y), \quad \phi = \phi(x, y) \tag{1}$$

where ϕ is electrical potential. The differential governing equation can be written as

$$c_{44}\nabla^2 u_z + e_{15}\nabla^2 \phi = 0, \quad e_{15}\nabla^2 u_z - \kappa_{11}\nabla^2 \phi = 0 \quad \text{in} \quad \Omega \tag{2}$$

with the constitutive equations

$$\begin{Bmatrix} \sigma_{xz} \\ \sigma_{yz} \\ D_x \\ D_y \end{Bmatrix} = \begin{bmatrix} c_{44} & 0 & -e_{15} & 0 \\ 0 & c_{44} & 0 & -e_{15} \\ e_{15} & 0 & \kappa_{11} & 0 \\ 0 & e_{15} & 0 & \kappa_{11} \end{bmatrix} \begin{Bmatrix} \gamma_{xz} \\ \gamma_{yz} \\ E_x \\ E_y \end{Bmatrix} \tag{3}$$

or

$$\begin{Bmatrix} \gamma_{xz} \\ \gamma_{yz} \\ E_x \\ E_y \end{Bmatrix} = \begin{bmatrix} s_{44} & 0 & g_{15} & 0 \\ 0 & s_{44} & 0 & g_{15} \\ -g_{15} & 0 & \lambda_{11} & 0 \\ 0 & -g_{15} & 0 & \lambda_{11} \end{bmatrix} \begin{Bmatrix} \sigma_{xz} \\ \sigma_{yz} \\ D_x \\ D_y \end{Bmatrix} \tag{4}$$

where c_{44} is an elastic stiffness constant measured in a constant electric field while κ_{11} stands for the dielectric constant measured at constant strain, e_{15} is the piezoelectric constant, $\nabla^2 = \partial^2/\partial x^2 + \partial^2/\partial y^2$ is the two-dimensional Laplace operator σ_{xz} and σ_{yz}, are the shear stresses, D_x and D_y are the x- and y-components of electric displacement, γ_{xz}, γ_{yz} and E_x, E_y are, respectively, shear strains and electric fields given by

$$\gamma_{xz} = \frac{\partial u_z}{\partial x}, \quad \gamma_{yz} = \frac{\partial u_z}{\partial y}, \quad E_x = -\frac{\partial \phi}{\partial x}, \quad E_y = -\frac{\partial \phi}{\partial y} \tag{5}$$

The constants s_{44}, g_{15} and λ_{11} are defined by the relations:

$$s_{44} = \frac{\kappa_{11}}{\Delta}, \quad g_{15} = \frac{e_{15}}{\Delta}, \quad \lambda_{11} = \frac{c_{44}}{\Delta}, \quad \Delta = c_{44}\kappa_{11} + e_{15}^2 \tag{6}$$

The boundary conditions of the boundary value problem (1)-(5) can be given by:

$$u_z = \bar{u}_z \quad \text{on } \Gamma_u \tag{7}$$

$$t = \sigma_{3j} n_j = \bar{t} \quad \text{on } \Gamma_t \tag{8}$$

$$D_n = D_i n_i = -\bar{\omega}_n = \bar{D}_n \quad \text{on } \Gamma_D \tag{9}$$

$$\phi = \bar{\phi} \quad \text{on } \Gamma_\phi \tag{10}$$

where $\bar{u}, \bar{t}, \bar{\omega}_n$ are $\bar{\phi}$, respectively, prescribed boundary displacement, traction force, surface charge and electric potential, an overhead bar denotes prescribed value, $\Gamma = \Gamma_u + \Gamma_t = \Gamma_D + \Gamma_\phi$ is the boundary of the solution domain Ω.

It is obvious from Eq. (2) that it requires

$$c_{44}\kappa_{11} + e_{15}^2 \neq 0 \tag{11}$$

to have a non-trivial solution for the out-of-plane displacement and in-plane electric fields. It results in

$$\nabla^2 u_z = 0, \quad \nabla^2 \phi = 0 \tag{12}$$

2.2 Trefftz functions

It is well known that the solutions of the Laplace Eq. (12) may be found using the method of variable separation. By this method, the Trefftz functions are obtained as Qin (2000)

$$u_z(r, \theta) = \sum_{m=0}^{\infty} r^m (a_m \cos m\theta + b_m \sin m\theta) \tag{13}$$

$$\phi(r, \theta) = \sum_{m=0}^{\infty} r^m (c_m \cos m\theta + d_m \sin m\theta) \tag{14}$$

for a bounded region and

$$u_z(r, \theta) = a_0^* + a_0 \ln r + \sum_{m=1}^{\infty} r^{-m} (a_m \cos m\theta + b_m \sin m\theta) \tag{15}$$

$$\phi(r, \theta) = c_0^* + c_0 \ln r + \sum_{m=1}^{\infty} r^{-m} (c_m \cos m\theta + d_m \sin m\theta) \tag{16}$$

for an unbounded region, where r and θ are a pair of polar coordinates. Thus, the associated T-complete sets of Eqs. (13)-(16) can be expressed in the form

$$N = \{1, r\cos\theta, r\sin\theta, \ldots, r^m \cos m\theta, r^m \sin m\theta, \ldots\} = \{N_i\} \tag{17}$$

$$N = \{1, \ln r, r^{-1}\cos\theta, r^{-1}\sin\theta, \ldots, r^{-m}\cos m\theta, r^{-m}\sin m\theta, \ldots\} = \{N_i\} \tag{18}$$

2.3 Particular solution for a subdomain containing angular corner

It is well known that singularities induced by local defects such as angular corners, cracks, and so on, can be accurately accounted for in the conventional FE or BEM model by way of appropriate

local refinement of the element mesh. However, an important feature of the Trefftz method is that such problems can be far more efficiently handled by the use of particular solutions (Qin 2000). In this sub-section we will show how particular solutions can be constructed to satisfy both the Laplace Eq. (12) and the traction-free boundary conditions on angular corner faces (Fig. 1). The derivation of such functions is based on the general solution of the two-dimensional Laplace equation:

$$u_z(r, \theta) = a_0 + \sum_{n=1}^{\infty} (a_n r^{\lambda_n} + c_n r^{-\lambda_n})\cos(\lambda_n \theta) + \sum_{n=1}^{\infty} (d_n r^{\lambda_n} + g_n r^{-\lambda_n})\sin(\lambda_n \theta) \tag{19}$$

$$\phi(r, \theta) = b_0 + \sum_{n=1}^{\infty} (b_n r^{\lambda_n} + f_n r^{-\lambda_n})\cos(\lambda_n \theta) + \sum_{n=1}^{\infty} (e_n r^{\lambda_n} + h_n r^{-\lambda_n})\sin(\lambda_n \theta) \tag{20}$$

Appropriate trial functions for a sub-domain containing a singular corner are obtained by considering an infinite wedge (Fig. 1) with particular boundary conditions prescribed along the sides $\theta = \pm\theta_0$ forming the angular corner. The boundary conditions on the upper and lower surfaces of the wedge are free of surface traction and surface charge:

$$\sigma_{z\theta} = c_{44}\frac{\partial u_z}{r\partial\theta} + e_{15}\frac{\partial \phi}{r\partial\theta} = 0, \quad D_\theta = e_{15}\frac{\partial u_z}{r\partial\theta} - \kappa_{11}\frac{\partial \phi}{r\partial\theta} = 0 \tag{21}$$

This leads to

$$\frac{\partial u_z}{\partial\theta} = 0, \quad \frac{\partial \phi}{\partial\theta} = 0 \quad (\text{for} \quad \theta = \pm\theta_0) \tag{22}$$

Considering the symmetry of free boundary condition on x_1-axis of the singular corner and the different properties of sin- and cos- functions, which should depend on different variables in order to satisfy the same boundary conditions, introduce a set of new constants β_n and rewrite the general solutions (19) as

$$u_z(r, \theta) = a_0 + \sum_{n=1}^{\infty} (a_n r^{\lambda_n} + c_n r^{-\lambda_n})\cos(\lambda_n \theta) + \sum_{n=1}^{\infty} (d_n r^{\beta_n} + g_n r^{-\beta_n})\sin(\beta_n \theta) \tag{23}$$

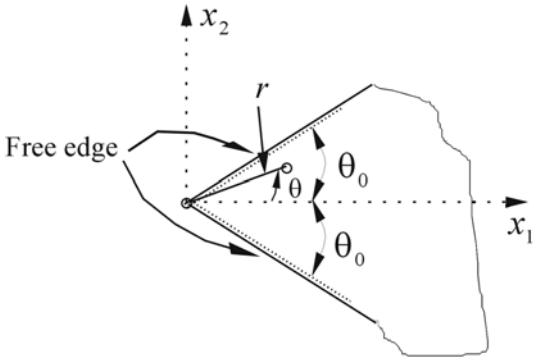

Fig. 1 Typical subdomain containing a singular corner

where λ_n and β_n are two sets of constants which are assumed to be greater than zero. Differentiating the solution (23) and substituting it into Eq. (22) yields

$$\left.\frac{\partial u_z}{\partial \theta}\right|_{\theta=\pm\theta_0} = -\sum_{n=1}^{\infty} \lambda_n (a_n r^{\lambda_n} + c_n r^{-\lambda_n}) \sin(\pm\lambda_n \theta_0)$$

$$+ \sum_{n=1}^{\infty} \beta_n (d_n r^{\beta_n} + g_n r^{-\beta_n}) \cos(\pm\beta_n \theta_0) = 0 \tag{24}$$

Since the solution must be limited for $r = 0$, we should specify

$$c_n = g_n = 0 \tag{25}$$

From Eq. (24) it can be deduced that

$$\sin(\pm\lambda_n \theta_0) = 0, \quad \cos(\pm\beta_n \theta_0) = 0 \tag{26}$$

leading to

$$\lambda_n \theta_0 = n\pi \quad (n = 1, 2, 3, \ldots) \tag{27}$$

$$2\beta_n \theta_0 = n\pi \quad (n = 1, 3, 5, \ldots) \tag{28}$$

Thus, for an element containing an edge crack (in this case $\theta_0 = \pi$), the solution can be written in the form

$$u_z(r, \theta) = a_0 + \sum_{n=1}^{\infty} a_n r^n \cos(n\theta) + \sum_{n=1,3,5}^{\infty} d_n r^{\frac{n}{2}} \sin\left(\frac{n}{2}\theta\right) = \sum_{n=1}^{\infty} a_n r_n^* + \sum_{n=1,3,5}^{\infty} d_n f_n^* \tag{29}$$

where $r_n^* = r^n \cos(n\theta)$ and $f_n^* = r^{\frac{n}{2}} \sin\left(\frac{n}{2}\theta\right)$

It is obvious that the displacement function (29) includes the term proportional to $r^{1/2}$, whose derivative is singular at the crack tip. The solution for the second equation of (22) can be obtained similarly and denoted as

$$\phi(r, \theta) = b_0 + \sum_{n=1}^{\infty} b_n r^n \cos(n\theta) + \sum_{n=1,3,5}^{\infty} e_n r^{\frac{n}{2}} \sin\left(\frac{n}{2}\theta\right) = \sum_{n=1}^{\infty} b_n r_n^* + \sum_{n=1,3,5}^{\infty} e_n f_n^* \tag{30}$$

Thus, the associated T-complete sets of Eqs. (29) and (30) can be expressed in the form

$$N = \left\{1, r\cos\theta, r^{\frac{1}{2}} \sin\left(\frac{\theta}{2}\right), \ldots, r^m \cos m\theta, r^{\frac{2m-1}{2}} \sin\left(\frac{2m-1}{2}\theta\right), \ldots\right\} = \{N_i\} \tag{31}$$

2.4 Stress intensity factor

Generally, stress intensity factors (SIF) can be evaluated by analysing stress and displacement

fields near crack-tips using various numerical methods such as conventional FEM and boundary element method. These procedures are usually complicated and time-consuming as they cannot calculate the SIF directly from basic variables like the coefficients d_i and e_i. But in the light of the special purpose function for crack-tip element, it can be easily to obtain local field distribution in crack problem, such as stress and electric displacement fields. Hence, high efficiency in solving singular problem by HTBE approach is the attractive possibility of straightforwardly by evaluating SIF K_{III} and K_D from d_i and e_i, which are associated with the singular factors in particular solutions (29) and (30). To show this, considering the $r^{-1/2}$ type of stress singularity the corresponding SIF K_{III} can be defined as

$$\sigma_{32} = \frac{K_{III}}{\sqrt{2\pi r}}\cos\frac{\theta}{2} \Rightarrow K_{III} = \lim_{r\to 0}\sqrt{2\pi r}\,\sigma_{32}/\cos\frac{\theta}{2} \tag{32}$$

and when $\theta = 0$

$$K_{III} = \lim_{r\to 0}\sqrt{2\pi r}\,\sigma_{32} \tag{33}$$

Substituting Eqs. (4), (5), and (29) into Eq. (33), we have

$$K_{III} = \lim_{r\to 0}\sqrt{2\pi r}\left\{\sum_{n=1}^{\infty}(c_{44}a_n + e_{15}b_n)\frac{\partial r_n^*}{\partial y} + \sum_{n=1,3,5}^{\infty}(c_{44}d_n + e_{15}e_n)\frac{\partial f_n^*}{\partial y}\right\} \tag{34}$$

When the cracks tip is defined at the origin of the polar coordinate system (see Fig. 1), Eq. (34) can be written as

$$K_{III} = \lim_{r\to 0}\frac{\sqrt{2\pi r}}{r}\left\{\sum_{n=1}^{\infty}(c_{44}a_n + e_{15}b_n)\frac{\partial r_n^*}{\partial \theta} + \sum_{n=1,3,5}^{\infty}(c_{44}d_n + e_{15}e_n)\frac{\partial f_n^*}{\partial \theta}\right\} \tag{35}$$

Substituting Eq. (35) into Eq. (34), it can be obtained the expression of stress singular factor

$$K_{III} = \sqrt{\frac{\pi}{2}}(c_{44}d_1 + e_{15}e_1) \tag{36}$$

In general, when $\theta_0 \neq \pi$, the singularity become the type of $r^{\lambda-1}$, where $\lambda = 1 - \pi/2\theta_0$, we can have general expression of stress singularity corresponding stress intensity factors are defined as

$$K_{III} = \lim_{r\to 0}\left[\frac{(2\pi)^{1/2}}{r^{1-\lambda}}\sigma_{32}(r,0)\right] \tag{37}$$

and it can be also written as:

$$K_{III} = \sqrt{2\pi}(c_{44}d_1 + e_{15}e_1)\frac{\pi}{2\theta_0} \tag{38}$$

Similarly, the singularity factor K_D can also be written as

$$K_D = \sqrt{2\pi}(e_{15}d_1 - \kappa_{11}e_1)\frac{\pi}{2\theta_0} \tag{39}$$

3. Indirect formulation

In the indirect method, the unknown displacement u_z and electric potential ϕ are approximated by the expansions as

$$\mathbf{u} = \begin{Bmatrix} u_z \\ \phi \end{Bmatrix} = \sum_{j=0}^{m} \begin{bmatrix} N_{1j} & 0 \\ 0 & N_{2j} \end{bmatrix} \begin{Bmatrix} c_{uj} \\ c_{\phi j} \end{Bmatrix} = \begin{bmatrix} \mathbf{N}_1 \\ \mathbf{N}_2 \end{bmatrix} \mathbf{c} = \mathbf{N}\mathbf{c} \tag{40}$$

where N_i is taken from Eq. (17) for subdomains without crack or Eq. (31) for the remaining, and $\mathbf{c}$ denote the unknown vector. Using the definitions (3), (5), (8) and (9), the generalized boundary force and electric displacements can be given by

$$\mathbf{T} = \begin{bmatrix} t \\ D_n \end{bmatrix} = \begin{Bmatrix} \sigma_{3j} n_j \\ D_j n_j \end{Bmatrix} = \begin{bmatrix} \mathbf{Q}_1 \\ \mathbf{Q}_2 \end{bmatrix} \mathbf{c} = \mathbf{Q}\mathbf{c} \tag{41}$$

With the expressions above, the indirect formulation corresponding to the anti-plane problem can be expressed by

$$\int_{\Gamma_u} (\bar{u}_z - u_z) w_1 ds + \int_{\Gamma_\phi} (\bar{\phi} - \phi) w_2 ds + \int_{\Gamma_t} (\bar{t} - t) w_3 ds + \int_{\Gamma_D} (\bar{D}_n - D_n) w_4 ds \tag{42}$$

where w_i (i = 1-4) are arbitrary weighting functions and u_z, ϕ, t, D_n have the series representations (40) and (41). If we use Galerkin method, the weighting functions are chosen as arbitrary variations of the expressions (40) and (41), that is:

$$w_1 = \mathbf{Q}_1 \delta\mathbf{c}, \quad w_2 = \mathbf{Q}_2 \delta\mathbf{c}, \quad w_3 = -\mathbf{N}_1 \delta\mathbf{c}, \quad w_4 = -\mathbf{N}_2 \delta\mathbf{c} \tag{43}$$

Substituting Eq. (43) into Eq. (42), yields

$$\mathbf{K}\mathbf{c} = \mathbf{f} \tag{44}$$

where

$$\mathbf{K} = \int_{\Gamma_u} \mathbf{Q}_1^T \mathbf{N}_1 ds - \int_{\Gamma_t} \mathbf{N}_1^T \mathbf{Q}_1 ds + \int_{\Gamma_\phi} \mathbf{Q}_2^T \mathbf{N}_2 ds - \int_{\Gamma_D} \mathbf{N}_2^T \mathbf{Q}_2 ds \tag{45}$$

$$\mathbf{f} = \int_{\Gamma_u} \mathbf{Q}_1^T \bar{u}_z ds - \int_{\Gamma_t} \mathbf{N}_1^T \bar{t}\, ds + \int_{\Gamma_\phi} \mathbf{Q}_2^T \bar{\phi} ds - \int_{\Gamma_D} \mathbf{N}_2^T \bar{D}_n ds \tag{46}$$

It is noted that the formulation above applys only to the solution domain containing one semi-infinite crack when the particular solution (31) is used as the weighting function. For multi-crack problem, the domain decomposition approach is required. In this case, the solution domain is divided into several sub-domains (Fig. 2). For example, the domain containing two cracks can be divided into four sub-domains (Fig. 2), In the figure, Ω_i (i = 1-4) denote the sub-domains, Γ outer boundary, and Γ_{Iij} the inner boundaries between sub-domains. For each sub-domain, the indirect method leads to

$$\mathbf{K}_i \mathbf{c}_i = \mathbf{f}_i \quad (i = 1\text{-}4) \tag{47}$$

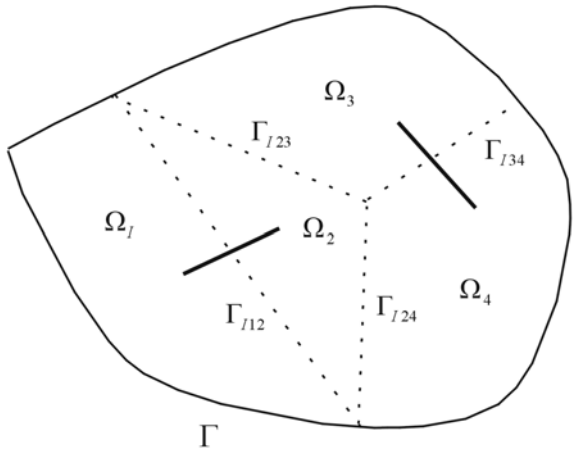

Fig. 2 Four sub-domain problem

On the inner boundary Γ_{Iij}, the continuity conditions provides

$$u_{zI}^i = u_{zI}^j, \quad \phi_I^i = \phi_I^j, \quad t_I^i = -t_I^j, \quad D_{nI}^i = -D_{nI}^j \tag{48}$$

where the subscript I stand for the inner boundary, and superscript i (or j) means the ith (or jth) subdomain. Eqs. (47) and (48) can be used to solve multiple crack problems.

4. Direct formulation

The Trefftz direct formulation is obtained by considering (Cheung *et al.* 1989, Kita *et al.* 1999)

$$\iint_\Omega [\nabla^2 u_z v_1 + \nabla^2 \phi v_2] d\Omega = 0 \tag{49}$$

Performing the integration by parts and taking the expression (40) as weighting function, that is:

$$\mathbf{v} = \begin{Bmatrix} v_1 \\ v_2 \end{Bmatrix} = \sum_{j=0}^{m} \begin{bmatrix} N_{1j} & 0 \\ 0 & N_{2j} \end{bmatrix} \begin{Bmatrix} c_{uj} \\ c_{\phi j} \end{Bmatrix} = \begin{bmatrix} \mathbf{N}_1 \\ \mathbf{N}_2 \end{bmatrix} \mathbf{c} = \mathbf{N}\mathbf{c} \tag{50}$$

we have,

$$\mathbf{c}^T \int_\Gamma (\mathbf{N}_1^T t - \mathbf{Q}_1^T u_z + \mathbf{N}_2^T D_n - \mathbf{Q}_2^T \phi) ds = 0 \tag{51}$$

Since the equation is valid for arbitrary vectors $\mathbf{c}$, we have

$$\int_\Gamma (\mathbf{N}_{1i}^T t - \mathbf{Q}_{1i}^T u_z + \mathbf{N}_{2i}^T D_n - \mathbf{Q}_{2i}^T \phi) ds = 0 \tag{52}$$

The analytical results for the Eq. (52) are, in general, impossible, and therefore a numerical procedure must be used to solve the problem. As in the conventional boundary element method, the

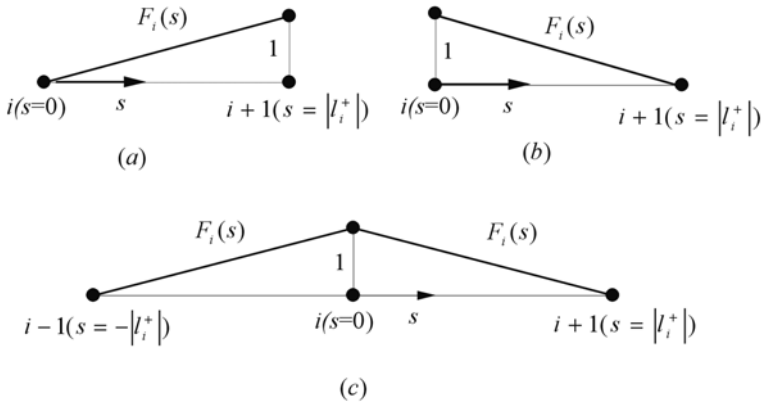

Fig. 3 Definitions of $F_i(s)$, $|l_i^+|$, $|l_i^-|$

boundary Γ is divided into m linear elements, for which u_z, t, ϕ, and D_n are approximated by

$$u_z(s) = \sum_{i=1}^{m} u_{zi}F_i(s), \quad t(s) = \sum_{i=1}^{m} t_iF_i(s), \quad \phi(s) = \sum_{i=1}^{m} \phi_iF_i(s), \quad D_n(s) = \sum_{i=1}^{m} D_{ni}F_i(s) \tag{53}$$

where u_{zi}, t_i, ϕ, and D_n are, respectively, their values at node i. $s>0$ in the element located at the right of the node i, $s<0$ in the element located at the left of the node. $F_i(s)$ is a global shape function associated with the ith-node. $F_i(s)$ is zero-valued over the whole mesh except within two elements connected to the ith-node (see Fig. 3). Since $F_i(s)$ is assumed to be linear within each element, it has below three possible forms:

$$F_i(s) = (|l_i^+| - s)/|l_i^+| \tag{54}$$

for a node located at the left end of a line (see Fig. 3a), or

$$F_i(s) = (|l_i^-| + s)/|l_i^-| \tag{55}$$

for a node located at the right end of a line (see Fig. 3b), or

$$F_i(s) = \begin{cases} (|l_i^-| + s)/|l_i^-| & \text{if } s \in l_i^- \\ (|l_i^+| - s)/|l_i^+| & \text{if } s \in l_i^+ \end{cases} \tag{56}$$

where l_i^+ are l_i^- the two elements connected to the ith node, l_i^+ being to the right and l_i^- being to the left, while $|l_i^+|$ and $|l_i^-|$ denote their length, and

$$s = \begin{cases} 0 & \text{at node } i \\ |l_i^+| & \text{at node } i+1 \\ |-l_i^-| & \text{at node } i-1 \end{cases} \tag{57}$$

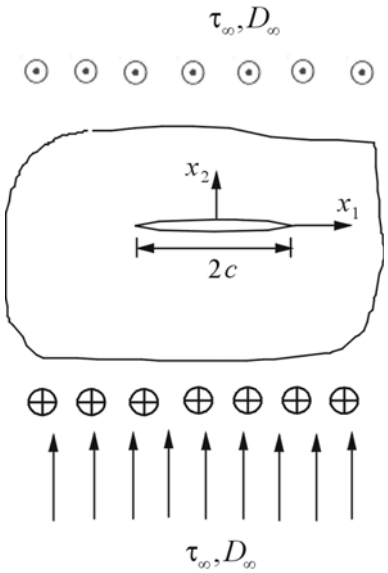

Fig. 4 Configuration of the cracked infinite piezoelectric medium

Having performed discretion above, yields

$$\mathbf{Gu} = \mathbf{Ht} \tag{58}$$

Applying the boundary conditions, we have

$$[\mathbf{G}_1 \ \mathbf{G}_2 \ \mathbf{G}_3 \ \mathbf{G}_4]\begin{Bmatrix} \bar{\mathbf{u}}_z \\ \mathbf{u}_z \\ \bar{\varphi} \\ \varphi \end{Bmatrix} = [\mathbf{H}_1 \ \mathbf{H}_2 \ \mathbf{H}_3 \ \mathbf{H}_4]\begin{Bmatrix} \bar{\mathbf{t}} \\ \mathbf{t} \\ \bar{\mathbf{D}}_n \\ \mathbf{D}_n \end{Bmatrix} \tag{59}$$

or simply

$$\mathbf{Kx} = \mathbf{f} \tag{60}$$

The direct formulation above is only suitable for single crack problem. For multi-crack problem, as was treated in Section 3, the domain decomposition approach is used to convert it into several single crack problems. For a particular single crack problem with sub-domain i (see Fig. 2), Eq. (60) becomes

$$\mathbf{K}_i\mathbf{x}_i = \mathbf{f}_i \quad \text{in } \Omega_i \tag{61}$$

While on the inner boundary Γ_{Iij}, the continuity condition is again defined in Eq. (48).

5. Numerical example

As a numerical illustration of the proposed formulation, two simple examples are considered. In order to allow for comparisons with analytical results, which appeared in (Zhou and Wang 2001,

Qin 2003), the obtained results are limited to a central cracked piezoelectric plate (Qin 2003) and a piezoelectric strip with two collinear cracks along the x-axis of the strip (Zhou and Wang 2001). In all the calculations, The PZT-5H piezoelectric ceramic materials is used, the material constants of which are (Qin 2001) $c_{44} = 3.53 \times 10^{10}$ N/m^2, $e_{15} = 17.0$ C/m^2, $\kappa_{11} = 1.51 \times 10^{-8}$ C/(Vm), $J_{cr} = 5.0$ N/m where J_{cr} is the critical energy release rate.

Example 1: we consider an anti-plane crack of length $2c$ embedded in an infinite PZT-5H medium which is subjected to a uniform shear traction, $\sigma_{zy} = \tau_\infty$, and a uniform electric displacement, $D_y = D_\infty$ at infinity (see Fig. 4). In the Trefftz BE calculation, only one half of the geometry configuration shown in Fig. 5 is used due to the symmetry of the problem and a typical boundary element mesh is shown in Fig. 6. The energy release rate for PZT-5H material with a crack of length $2c = 0.02$ m and $a/c = 14$ is plotted in Fig. 7 as a function of electrical load with the mechanical load fixed such that $J = J_{cr}$ at zero electric load. The results are compared with those

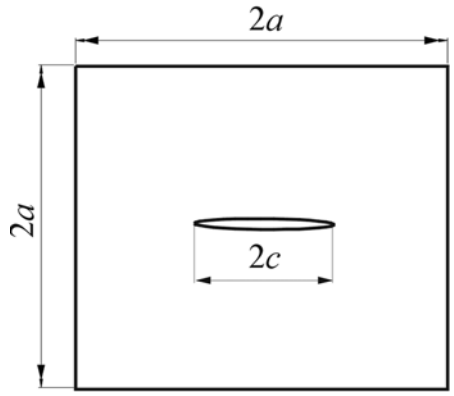

Fig. 5 Geometry of the cracked solid in numerical analysis

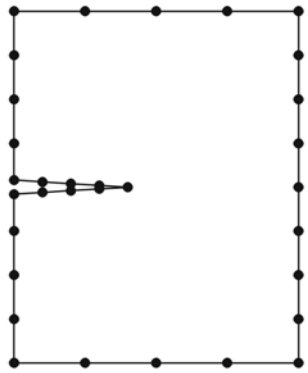

Fig. 6 A typical boundary mesh (32 elements)

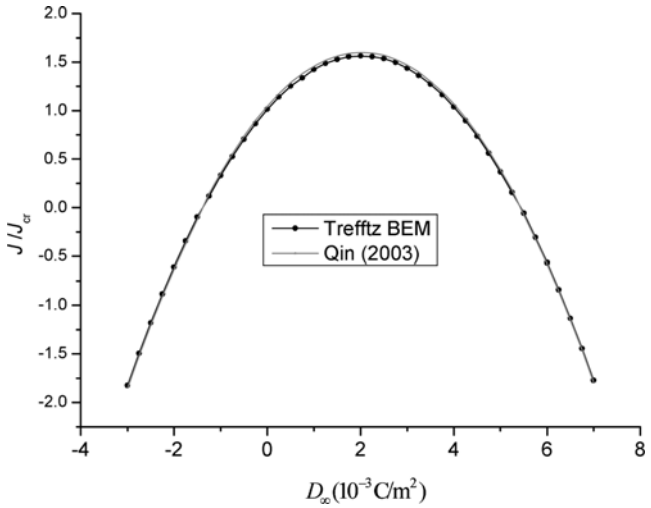

Fig. 7 Energy release rate in cracked PZT-5H plate ($a/c = 14$, $\tau_\infty = 4.2 \times 10^6$ N/m^2 and 32 elements)

Table 1 Boundary effect study on J/J_{cr} for central cracked piezoelectric plate ($D_\infty = 2 \times 10^{-3}$ C/m^2, and $\tau_\infty = 4.2 \times 10^{-6}$ N/m^2)

a/c	J/J_{cr}
6	1.5987
10	1.5922
14	1.5896
18	1.5895

Table 2 h-convergence study for J/J_{cr} for the central cracked piezoelectric plate ($a/c = 14$, $D_\infty = 2 \times 10^{-3}$ C/m^3, and $\tau_\infty = 4.2 \times 10^6$ N/m^2)

elements	J/J_{cr}
24	1.5961
32	1.5913
48	1.5901
64	1.5894
128	1.5893

Table 3 h-convergence study for K_{III}/K_{IIIS} and K_D/K_{DS} for the central cracked piezoelectric plate ($a/c = 14$, $D_\infty = 2 \times 10^{-3}$ C/m^3, and $\tau_\infty = 4.2 \times 10^6$ N/m^2)

elements	K_{III}/K_{IIIS}	K_D/K_{DS}
24	1.254	1.195
32	1.181	1.122
48	1.112	1.089
64	1.094	1.071
128	1.092	1.070

from Qin (2003). It is found from Fig. 7 that the energy release rate can be negative which means the crack growth may be arrested. It can also be found that there is a good agreement between two approaches although only 32 boundary elements have been used in the calculation. The energy release rate appeared in Fig. 7 was defined by Qin (2001)

$$J = G = \lim_{\Delta x \to 0} \frac{\Delta W}{\Delta x} \tag{61}$$

with

$$\Delta W = 2 \int_0^{\Delta x} \frac{1}{2} (\sigma_{zy} u_z + D_y \phi) dx \tag{62}$$

The boundary effect should be studied since we use a rectangular domain with side length $2a$ (see Fig. 5), rather than the infinite domain. The boundary effect is investigated by using different ratios of a/c (= 6, 10, 14, and 18). Numerical results of J/J_{cr} for different a/c are listed in Table 1. We found that the accuracy of the results is adequate when a/c is great than 14.

To study the convergent performance of the proposed formulation, numerical results of J/J_{cr} for different element meshes 24, 32, 48, 64, and 128 boundary elements are presented in Table 2 that the h-extension performs very nicely, and Table 3 shows the results of K_{III}/K_{IIIS} and K_D/K_{DS} for the

Table 4 J/J_{cr} for the central cracked piezoelectric plate from the two methods ($a/c = 14$, $D_\infty = 2 \times 10^{-3}$ C/m^3, and $\tau_\infty = 4.2 \times 10^6$ N/m^2)

Approach	Number of variables			
	48	64	96	128
Indirect method	1.5988	1.5924	1.5907	1.5901
Direct method	1.5961	1.5913	1.5901	1.5894

element meshes above. It also shows a good convergent performance, where (Qin 2001)

$$K_{IIIS} = c_{44}K_\gamma - e_{15}K_E, \quad K_{DS} = e_{15}K_\gamma + \kappa_{11}K_E \tag{63}$$

with

$$K_\gamma = \frac{\kappa_{11}\tau_\infty + e_{15}D_\infty}{c_{44}\kappa_{11} + e_{15}^2}\sqrt{\pi c}, \quad K_E = \frac{c_{44}D_\infty - e_{15}\tau_\infty}{c_{44}\kappa_{11} + e_{15}^2}\sqrt{\pi c} \tag{64}$$

Table 4 shows the results of J/J_{cr} obtained from both the indirect method and the direct method. It indicates that they have similar convergent performance. Therefore both of them are suitable for anti-plane fracture analysis although the values of J/J_{cr} obtained from the indirect method are slightly larger than those from the direct method.

Example 2: Consider a piezoelectric strip of width $2h(h = 2)$ which has an infinite extent in the y-z direction (see Fig. 8). Two collinear impermeable throuth cracks of equal length $(1 - b)$ along the x-axis (Zhou and Wang 2001). Here $2b$ is the distance between the two cracks. All two cracks are perpendicular to the edges of the strip. Assume that the strip be subjected to a constant shear stress, $\sigma_{32} = -\tau_0$, over the surface of the two cracks.

Owing to the symmetry of the problem only one half of the geometry configuration shown in Fig. 9 is analyzed and each subdomain (Ω_1 or Ω_2) is modelled by 64 boundary elements.

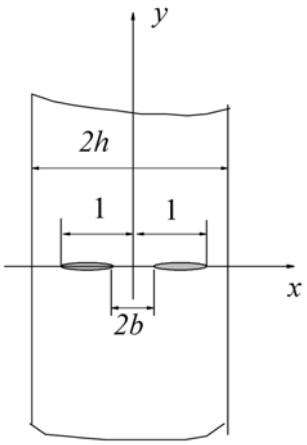

Fig. 8 Two cracks in a piezoelectric strip under anti-plane loading

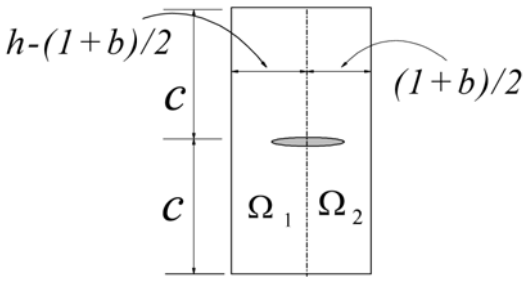

Fig. 9 Geometry of the two crack system in the Trefftz boundary element analysis

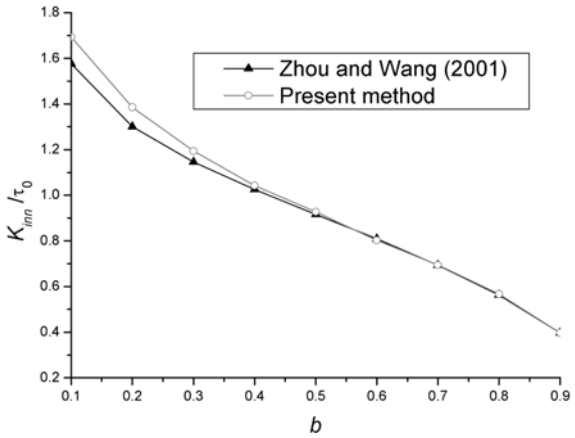

Fig. 10 K_{inn}/τ_0 vs crack distance b

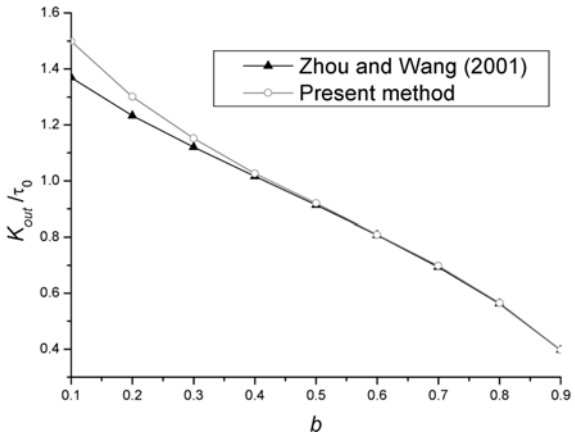

Fig. 11 K_{out}/τ_0 vs crack distance b

Figs. 10 and 11 display the variation of K_{inn}/τ_0 and K_{out}/τ_0 with the crack distance b, where c, K_{inn} and K_{out} are defined by Zhou and Wang (2001):

$$c = 12, \quad K_{inn} = \lim_{x \to b^+} \sqrt{2\pi(b+x)}\,\sigma_{32}(x,0), \quad K_{out} = \lim_{x \to -1^-} \sqrt{-2\pi(1+x)}\,\sigma_{32}(x,0)$$

It can be seen from Figs. 10 and 11 that the results from the present Trefftz BEM are in good agreement with analytical ones (Zhou and Wang 2001) when the crack distance b is greater than 0.4. However, discrepancy between the two methods will increase along with an decrease in b when b is less than 0.4. This indicates that edge effect will become important when the ratio of crack length $(1 - b)$ to the distance from the crack tip to the edge of the subdomain (b here) is great than 1.5, i.e., $(1 - b)/b > 1.5$. This result can help us to select the rational size of a subdomian when using the proposed formulation.

6. Conclusions

The Trefftz boundary element formulation for analysing anti-plane problems of piezoelectric materials has been developed. Special purpose functions for subdomians with a semi-infinite crack, satisfying exactly the crack-face condition, is proved to be useful in analysing stress singularity due to local effects. On the basis of the formulas presented in the paper and the Trefftz finite element model in Qin (2003), the energy release rate J/J_{cr} has been calculated and compared each other. The discrepancy between the two models is within 4%. The convergent performance of the proposed formulation was studied using several boundary element meshes and the results converge gradually to a certain value when the mesh density is increased. The results also show that the boundary effect can be ignored when a/c is great than 14. It can be seen from Table 4 that both the indirect method and the direct method have similar convergent performance and thus are suitable for anti-plane fracture analysis. The example for multi-crack problem is also considered here. The study shows that both the present Trefftz BEM and analytical solution (Zhou and Wang 2001) can provide almost the same results when the crack distance b is greater than 0.4.

Acknowledgements

The work was performed under the auspices of an Australian Professorial Fellowship Program with grant number DP0209487.

References

Cheung, Y.K., Jin, W.G. and Zienkiewicz, O.C. (1989), "Direct solution procedure for solution of harmonic problems using complete non-singular Trefftz functions", *Communi. Appl. Num. Meth.*, **5**, 159-169.

Domingues, J.S., Portela, A. and Castro, P.M.S.T. (1999), "Trefftz boundary element method applied to fracture mechanics", *Eng. Frac. Mech.*, **64**, 67-86.

Kita, E. and Kamiya, N. (1995), "Trefftz method: An overview", *Adv. Eng. Software*, **24**, 3-12.

Kita, E., Kamiya, N. and Iio, T. (1999), "Application of a direct Trefftz method with domain decomposition to 2D potential problems", *Eng. Analysis Bound. Elem.*, **23**, 539-548.

Pak, Y.E. (1990), "Crack extension force in a piezoelectric material", *J. Appl. Mech.*, **57**, 647-653.

Portela, A. and Charafi, A. (1997), "Trefftz boundary element methods for domains with slits", *Eng. Analysis Bound. Elem.*, **20**, 299-304.

Qin, Q.H. (2000), *The Trefftz Finite and Boundary Element Method*, WIT Press, Southampton, UK.

Qin, Q.H. (2001), *Fracture Mechanics of Piezoelectric Materials*, WIT Press, Southampton, UK.

Qin, Q.H. (2003), "Solving anti-plane problems of piezoelectric materials by the Trefftz finite element approach", *Computational Mechanics*, **31**, 461-468.

Sladek, J., Sladek, V. and Keer, Van R. (2002), "Global and local Trefftz boundary integral formulations", *Adv. Eng. Software*, **33**, 469-476.

Trefftz, E. (1926), "Ein Gegenstück zum Ritzschen Verfahren", *Proc. of 2nd Int. Congress of Applied Mechanics*, Zurich, 131-137.

Zhou, Z.G. and Wang, B. (2001), "Investigation of anti-plane shear behaviour of two collinear cracks in a piezoelectric materials strip by a new method", *Mech. Research Communi.*, **28**, 289-295.